Supplementary Information (SI) for CrystEngComm.

# A Triazolate-Based MOF with Amino-Induced Triazolate Reorientation Enabling Pore-Size Regulation for $CO_2/CH_4$ Separation

Qiyi Bu [a], Yushu Zhang [a,b], Jiaqi Liu [*b], Yong Wang [*a,b] and Jinping Li [a,b]

[a] College of Chemistry and Chemical Engineering, Taiyuan University of Technology, Taiyuan 030024, China.

[b] Shanxi Research Institute of Huairou Laboratory, Huazhang Street, Taiyuan, 030032, China.

Supporting Information

## Material and General characterization

All reagents were obtained from commercial suppliers and used as received. Single-crystal X-ray diffraction data were collected on a Bruker D8 VENTURE diffractometer equipped with a PHOTON II CPAD detector and a Ga-target Liquid METALJET D2 PLUS X-ray source with a wavelength of 1.34139 Å. Structural solutions were obtained using SHELXT (version 2018/2), followed by full-matrix least-squares refinement with SHELXL (version 2018/3) implemented in the OLEX2 graphical interface. Powder X-ray diffraction measurements were carried out on a Rigaku SmartLab SE diffractometer employing Cu-K alpha radiation (wavelength 1.5418 Å), with data collected over a 2 theta range from 3 to 40 degrees at a scan rate of 5 degrees per minute. The instrument was operated at 40 kV and 40 mA. Thermogravimetric analysis was conducted under a static nitrogen atmosphere using a NETZSCH simultaneous thermal analyzer with a heating rate of 10 °C per minute. Gas adsorption isotherms for single components were measured on a BK-300 volumetric adsorption analyzer. Prior to measurements, approximately 100 mg of sample was activated by evacuation at 120 °C for 5 hours. All gases employed in the adsorption experiments had a purity of 99.99%.

## Synthesis of $Zn_2(atz)_2$ipa-$NH_2$

$Zn(NO_3)_2·6H_2O$ (0.5 mmol), 3-amino-1,2,4-triazole (0.5 mmol), and 5-aminoisophthalic acid (0.5 mmol) were combined in a mixed solvent consisting of DMF and water (3 mL each) to form a homogeneous solution. The mixture was sealed in a 20 mL Teflon-lined stainless-steel autoclave and heated at 150 °C for 48 h. After the reaction vessel was cooled naturally to room temperature, colorless block-shaped crystals suitable for single-crystal X-ray diffraction were obtained. The resulting $Zn_2(atz)_2IPA\text{-}NH_2$ crystals were isolated by filtration and washed repeatedly with fresh DMF and water (five times each). Solvent exchange was then carried out using methanol in a Soxhlet extractor overnight. The sample was finally activated under dynamic vacuum at 120 °C for 12 h to afford the desolvated material.

## Topology analysis

The selection of node and linker was as follows:

V1 = Zn1; long distance represents isophthalic acid ligand; short distance represents triazole ligand

## Adsorption selectivity calculation

The dual site Langmuir-Freundlich isotherm model was adopted to fit the adsorption isotherms, which was described as follows:

$$q = q_{A,sat}\frac{b_A P^{v_A}}{1 + b_A P^{v_A}} + q_{B,sat}\frac{b_B P^{v_B}}{1 + b_B P^{v_B}} \tag{1}$$

with T-dependent parameters $b_A$, and $b_B$

$$b_A = b_{AO}\, exp\left(\frac{E_A}{RT}\right);\ b_B = b_{BO}\, exp\left(\frac{E_B}{RT}\right) \tag{2}$$

where $q$ represents the adsorption amount of adsorbents with units of mol·kg$^{-1}$, $q_{A,sat}$ and $q_{B,sat}$ represent the saturated adsorption amount for adsorption sites A and B, respectively, $b_A$ and $b_B$ are constants for species i at adsorption sites A and B, respectively, $p$ is the total pressure of the bulk gas at the adsorption equilibrium, and $v_A$ and $v_B$ are the Freundlich exponent for sites A and B, respectively.

the IAST selectivity is defined by:

$$S_{ads} = \frac{q_1/q_2}{y_1/y_2} \tag{3}$$

where $q_1$ and $q_2$ represents the adsorption amounts of $CO_2$ and $CH_4$ upon the sample under equilibrium condition, which are usually expressed with units of mmol·g$^{-1}$, $y_1$ and $y_2$ are the corresponding mole fractions in the gas phase for the mixtures. The calculated IAST adsorption selectivity for the $CH_4$ / $N_2$ (1/1; v/v) mixtures taking the mole fractions $y_1 = 0.5$ and $y_2 = 1\text{-}y_1 = 0.5$ for a total pressure of 101 kPa at 298 K.

## Multicomponent column breakthrough tests

Dynamic breakthrough measurements were performed on a laboratory-built fixed-bed adsorption system at 298 K and 1 bar. The composition of the effluent gas was continuously analyzed using a quadrupole mass spectrometer (Hidden HPR-20). For each experiment, approximately 0.81 g of $Zn_2(atz)_2IPA$ or 1.38 g of $Zn_2(atz)_2IPA\text{-}NH_2$ was loaded into a stainless-steel column with an inner diameter of 6 mm and a length of 100 mm. Prior to gas separation tests, the packed bed was activated under a helium flow of 10 mL per minute at 120 °C for 10 hours to eliminate residual solvents and adsorbed species. After activation, the column was allowed to cool to room temperature under helium. The helium flow was then discontinued, and a binary $CO_2$/$CH_4$ gas mixture was introduced at a total flow rate of 5 mL per minute. The breakthrough curves were collected continuously until dynamic adsorption equilibrium was achieved.

**Calculations and simulation details**

We used the DFT as implemented in the Vienna Ab initio simulation package (VASP) in all calculations. The exchange-correlation potential is described by using the generalized gradient approximation of Perdew-Burke-Ernzerhof (GGA-PBE). The projector augmented-wave (PAW) method is employed to treat interactions between ion cores and valence electrons. The plane-wave cutoff energy was fixed to 500 eV. Given structural models were relaxed until the Hellmann–Feynman forces smaller than -0.02 eV/Å and the change in energy smaller than $10^{-5}$ eV was attained. During the relaxation, the Brillouin zone was represented by a Γ centered k-point grid of 6×6×1. Grimme's DFT-D3 methodology was used to describe the dispersion interactions among all the atoms in adsorption models. Employing the climbing image nudged elastic band method (CI-NEB), we computed the minimum energy pathway of the diffuse reaction along with its corresponding activation barrier.

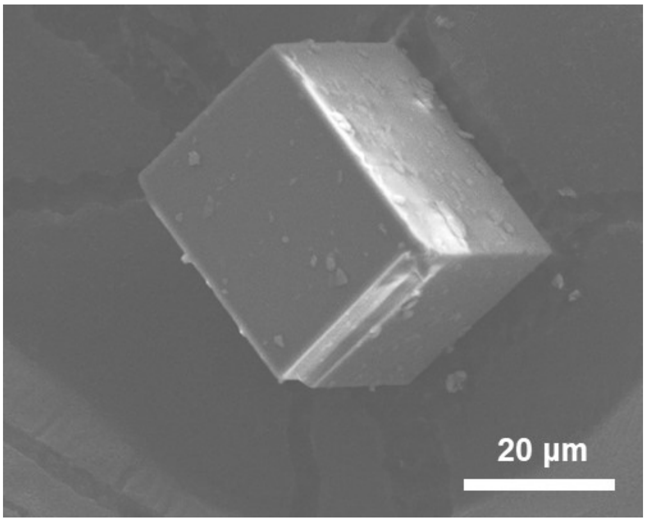

**Fig. S1** The scanning electron microscope image of the synthesized $Zn_2(atz)_2IPA\text{-}NH_2$-crystals.

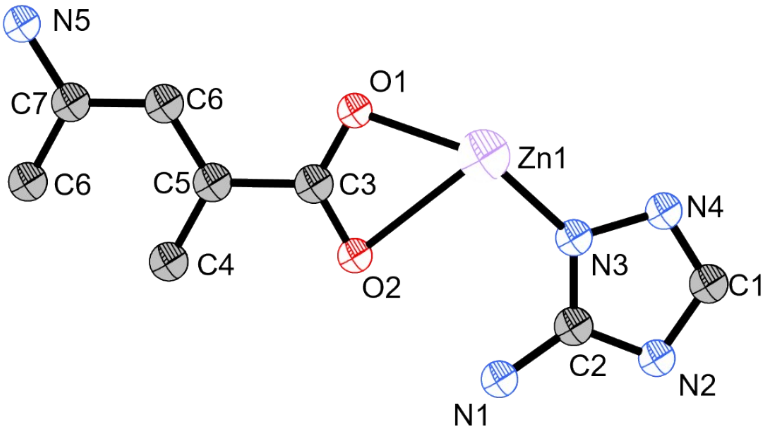

**Fig S2** The coordination environment of the independent Zn(II) ions in the crystal structure of $Zn_2(atz)_2IPA\text{-}NH_2$.

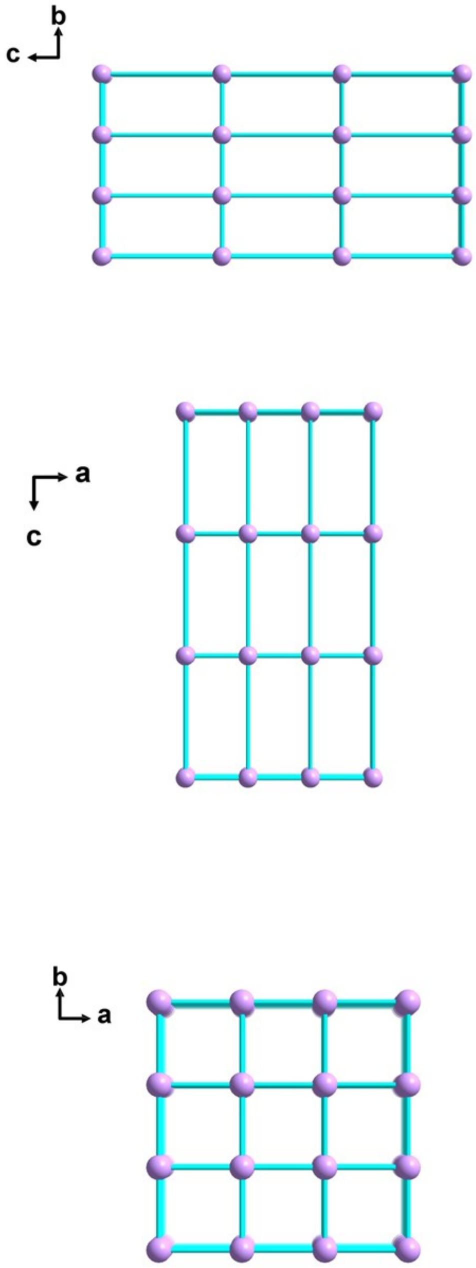

**Fig. S3** (a) The 3-D topological view of $Zn_2(atz)_2IPA\text{-}NH_2$. along *a* axis, (b) The 3-D topological view along *c* axis, (c) The 3-D topological view along *b* axis.

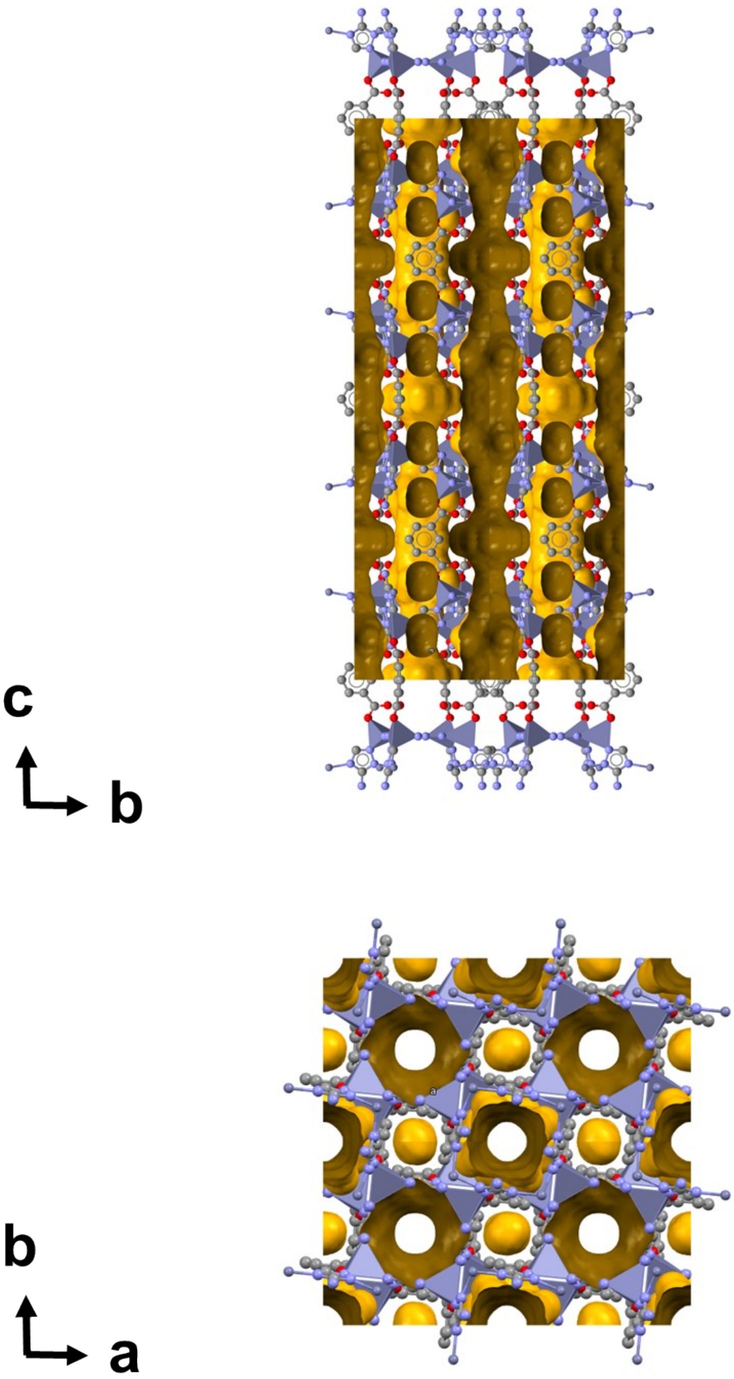

**Fig. S4** The pore structure of the as-synthesized $Zn_2(atz)_2IPA$ and $Zn_2(atz)_2IPA-NH_2$.

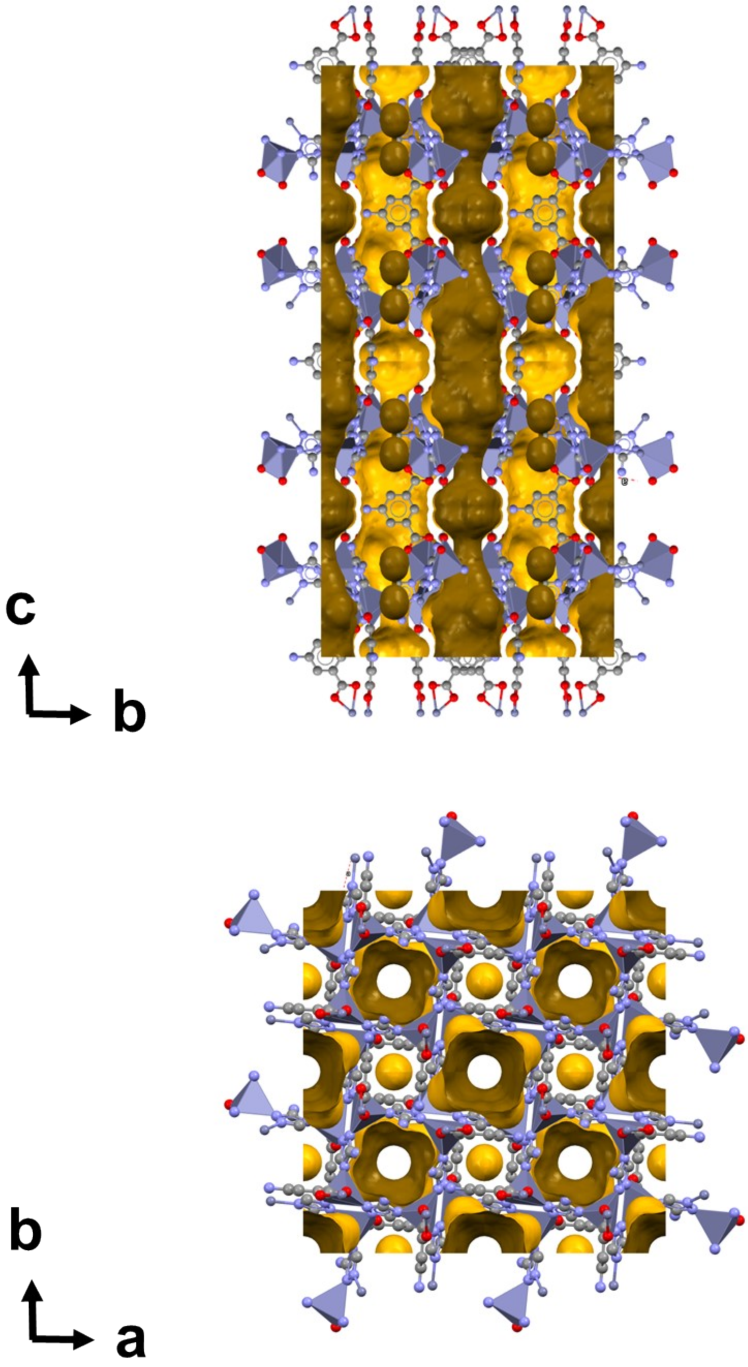

**Fig. S5** The pore structure of the as-synthesized $Zn_2(atz)_2IPA\text{-}NH_2$.

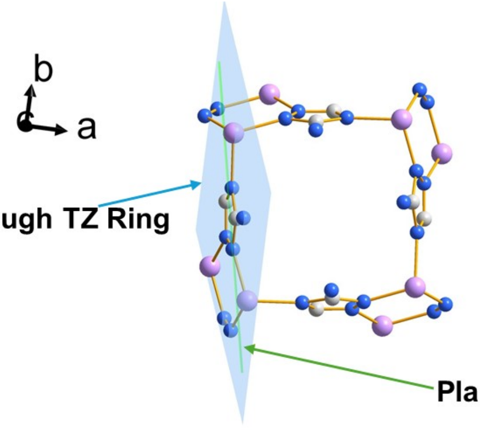

Plane 1: Through TZ Ring

Plane 2: Parallel to the b-axis, in the middle of TZ Ring

Angle between Plane1 and 2: 11.622°

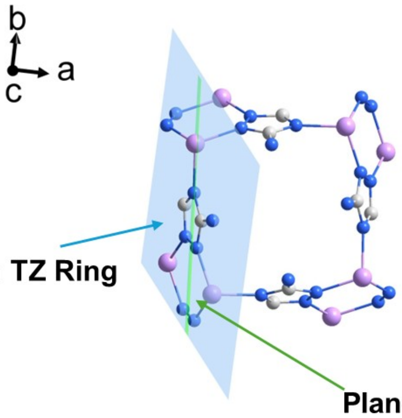

Plane 1: Through TZ Ring

Plane 2: Parallel to the b-axis, in the middle of TZ Ring

Angle between Plane1 and 2: 18.445°

**Fig. S6** The details of measurements for the angle between atz and the channel direction.

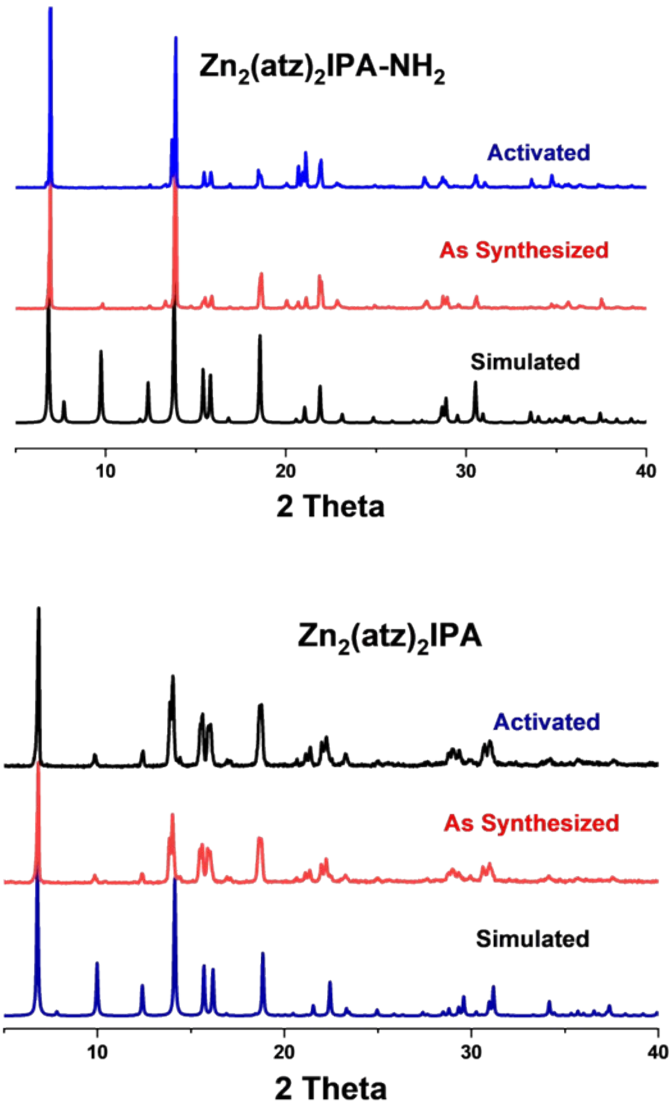

**Fig. S7** The comparison of PXRD patterns of the as-synthesized samples.

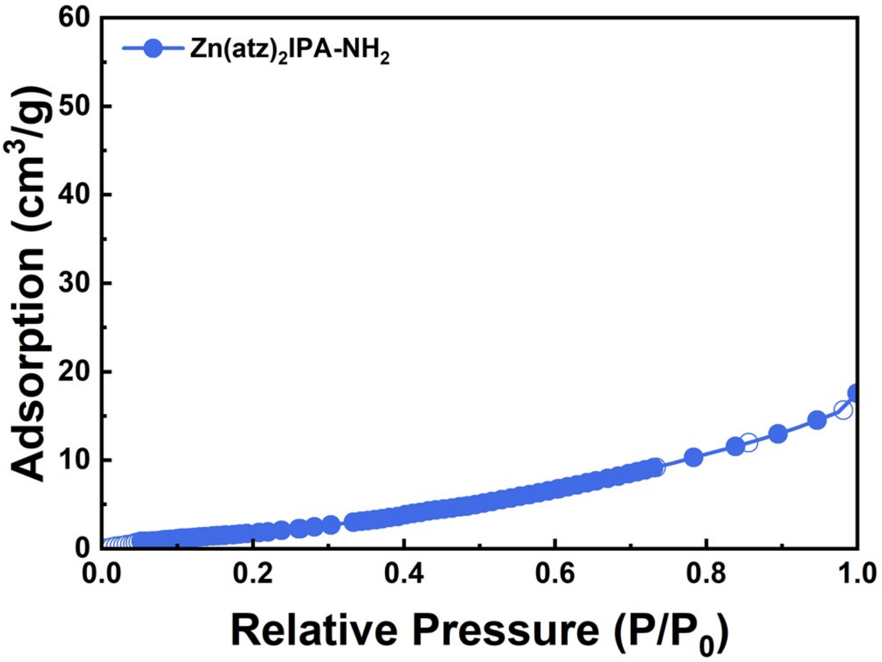

**Fig. S8** $N_2$ adsorption-desorption isotherms at 77 K on $Zn_2(atz)_2IPA\text{-}NH_2$.

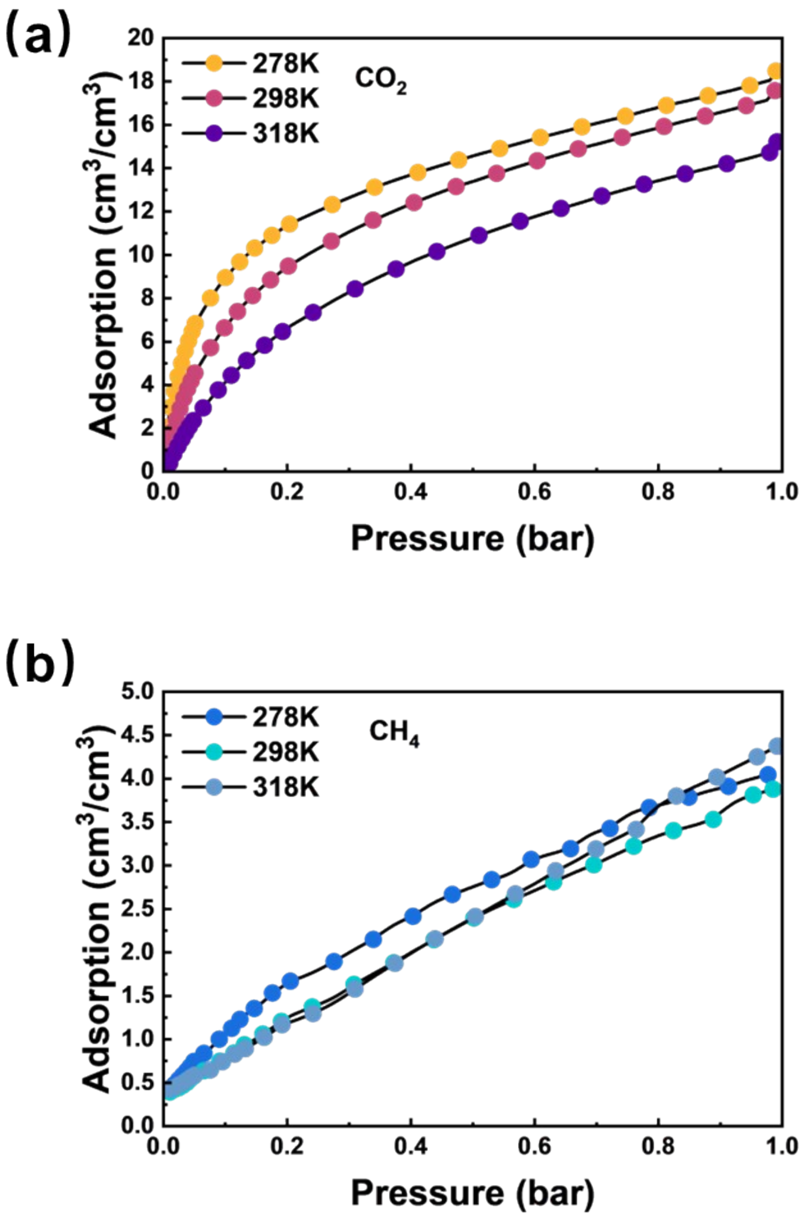

**Fig. S9** $CO_2$ (a) and $CH_4$ (b) adsorption-desorption isotherms at 278, 298 and 318 K on $Zn_2(atz)_2IPA\text{-}NH_2$.

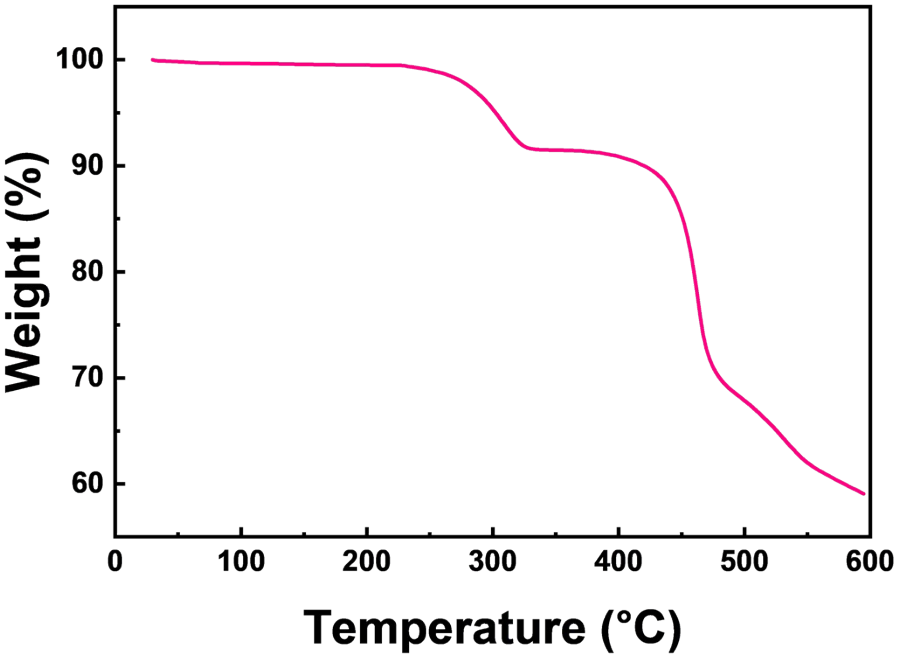

**Fig. S10** TG curve of $Zn_2(atz)_2IPA\text{-}NH_2$.

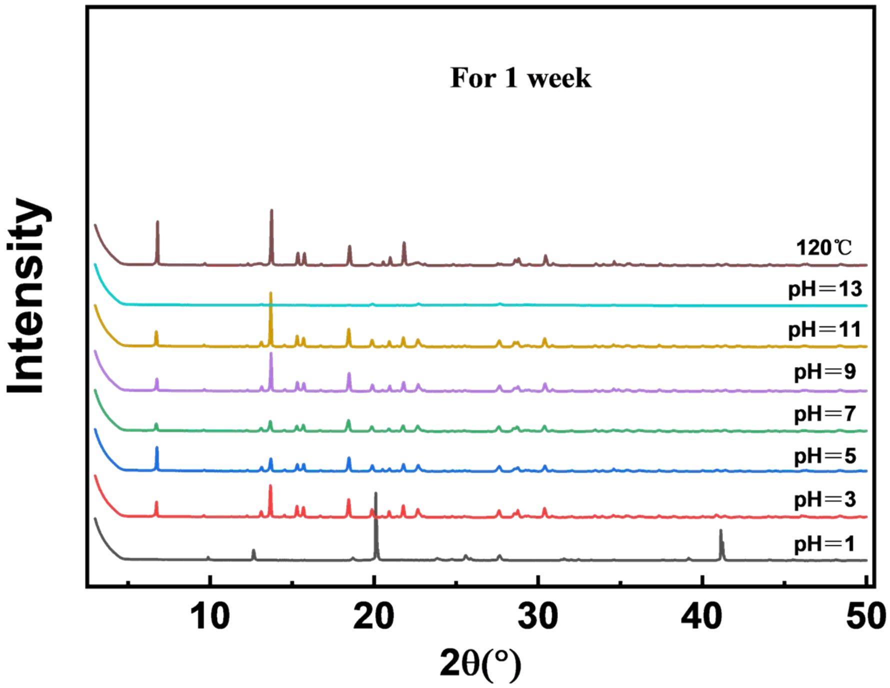

**Fig. S11** PXRD patterns of $Zn_2(atz)_2IPA\text{-}NH_2$ samples after being treated in different environments for 1 week.

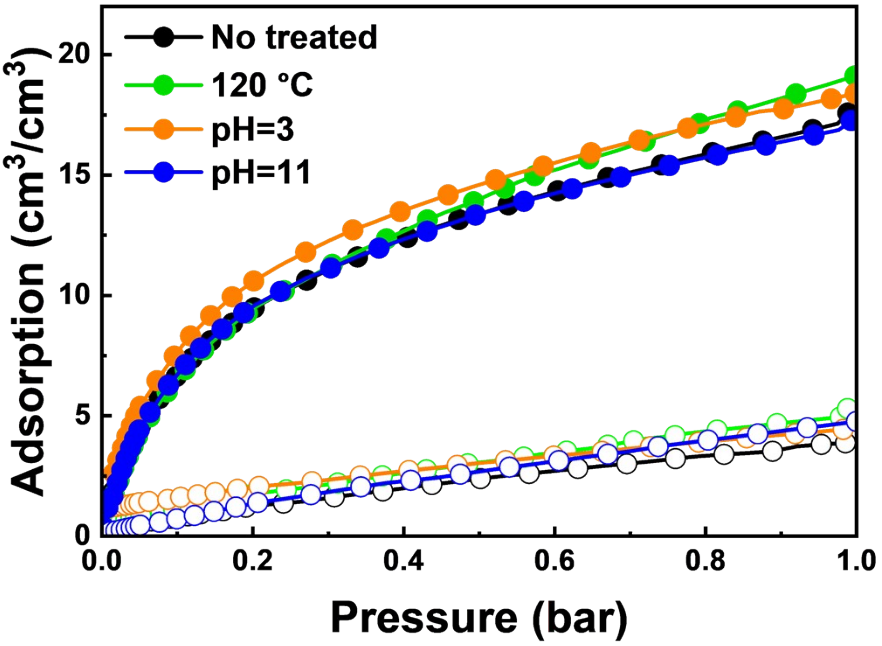

**Fig. S12** Adsorption isotherms for $CO_2$ and $CH_4$ after treatment for 1 week.

**Tab. S1** Crystal data and structure refinement.

| **Empirical formula** | $C_{12}H_{11}N_9O_4Zn_2$ |
|---|---|
| **Formula weight** | 476.04 |
| **Temperature/K** | 200.0 |
| **Crystal system** | tetragonal |
| **Space group** | I4/m |
| **a/Å** | 12.8268(8) |
| **b/Å** | 12.8268(8) |
| **c/Å** | 25.8853(19) |
| **α/°** | 90 |
| **β/°** | 90 |
| **γ/°** | 90 |
| **Volume/Å$^3$** | 4258.8(6) |
| **Z** | 8 |
| **$\rho_{calc}$g/cm$^3$** | 1.485 |
| **μ/mm$^{-1}$** | 3.088 |
| **F(000)** | 1904.0 |
| **Crystal size/mm$^3$** | 0.22 × 0.18 × 0.17 |
| **Radiation** | CuKα (λ = 1.54178) |
| **2Θ range for data collection/°** | 7.692 to 136.68 |
| **Index ranges** | $-13 \le h \le 15$, $-15 \le k \le 12$, $-31 \le l$ |
| **Reflections collected** | 8462 |
| **Independent reflections** | 1999 [Rint = 0.0483, Rsigma = |
| **Data/restraints/parameters** | 1999/5/138 |
| **Goodness-of-fit on F$^2$** | 1.086 |
| **Final R indexes [I>=2σ (I)]** | R1 = 0.0455, wR2 = 0.1408 |
| **Final R indexes [all data]** | R1 = 0.0500, wR2 = 0.1460 |
| **Largest diff. peak/hole / e Å$^{-3}$** | 0.36/-0.61 |

**Tab. S2** Fitting parameters of Dual-site Langmuir-Freundlich isotherm model for single gas adsorption at 298K.

| **$Zn_2(atz)_2IPA$** | Site A | | | Site B | | |
|---|---|---|---|---|---|---|
| | $q_{A,sat}$ $cm^3\ g^{-1}$ | $b_A$ $bar^{-1}$ | $v_A$ dimensionless | $q_{B,sat}$ $cm^3\ g^{-1}$ | $b_B$ $bar^{-1}$ | $v_B$ dimensionless |
| $CO_2$ | 10804.68 | 0.000435 | 1.077133 | 23.03874 | 4.764992 | 1.010612 |
| $CH_4$ | 17.63122 | 0.653958 | 1.184434 | 2.330821 | 6.93219 | 1.208276 |
| **$Zn_2(atz)_2IPA\text{-}NH_2$** | Site A | | | Site B | | |
| | $q_{A,sat}$ $cm^3\ g^{-1}$ | $b_A$ $bar^{-1}$ | $v_A$ dimensionless | $q_{B,sat}$ $cm^3\ g^{-1}$ | $b_B$ $bar^{-1}$ | $v_B$ dimensionless |
| $CO_2$ | 125784.2 | 1.65E-05 | 1.713519 | 11.87116 | 4.329155 | 0.853259 |
| $CH_4$ | 0.25087 | 8709947 | 3.367861 | 8.234608 | 0.406249 | 1.058575 |